

# Mechanism of voltage-sensitive fluorescence in a microbial rhodopsin

Dougal Maclaurin<sup>\*1</sup>, Veena Venkatachalam<sup>\*2</sup>, Hohjai Lee<sup>3</sup>, Adam E. Cohen<sup>1,3</sup>

<sup>(1)</sup>*Department of Physics*, <sup>(2)</sup>*Biophysics program*, <sup>(3)</sup>*Department of Chemistry and Chemical Biology, Harvard University, Cambridge, MA 02138*

cohen@chemistry.harvard.edu

## Supporting Information

### Supplementary Methods

#### Microscope system

The single-cell data shown in Figures 2, 3, and 4 were acquired on a homebuilt microscope, illustrated in Figure S2. Beams from four CW lasers (637 nm 100 mW Coherent OBIS; 594 nm 100 mW Cobolt Mambo; 532 nm 50 mW Coherent Compass 215M; 488 nm 50 mW Omicron PhoxX) were combined using dichroic mirrors and then spectrally selected using an acousto-optic tunable filter (AOTF; Gooch and Housego 48058). White light emission from a supercontinuum laser (Fianium SC-450-6) was spectrally selected using a second AOTF (Crystal Technologies). The polarization of the CW laser outputs was rotated 90° using an achromatic half wave plate (Thorlabs AQWP05M-600), and then combined with the CW laser outputs using a polarizing beam splitter. The intensity at each wavelength was controlled with 10  $\mu$ s time resolution.

Illumination was focused onto the back focal plane of the objective (Olympus, 1-U2B616 60 $\times$  oil, NA 1.45) via a 650 nm long-pass dichroic mirror. The sample was illuminated in epifluorescence mode and emission was collected by the same objective and passed through the dichroic mirror. Fluorescence was filtered with a 660 – 760 nm bandpass filter (Semrock) and collected on either a photomultiplier tube (PMT; Thorlabs PMM02 with multialkali (S20) photocathode) or a cooled EMCCD camera (Andor iXon X3 860, 128 x 128 pixels). The output of the photomultiplier tube was filtered at 50 kHz using an 8-pole Bessel filter (Alligator Technologies USBPGF-S1) and recorded at 100 kS/s on a National Instruments DAQ (PCIe-6323). The DAQ also produced control waveforms for the AOTF and patch-clamp amplifier, and recorded the patch-clamp current signals.

We measured laser intensities during experiments by splitting off a small fraction of the lasers onto a photodiode (Thorlabs DET36A). We accounted for the spectral response of the photodiode by calibrating against a well-calibrated power meter (Coherent FieldMax II). Due to the nonlinear intensity dependence of Arch photophysics, it was essential to ensure uniform illumination across the sample. To achieve this we expanded the Gaussian laser beams and selected a small region in the middle using an iris in an image plane to make a sharp disk of even illumination on our sample. We confirmed using a uniform sample of fluorescent beads (Invitrogen) that the intensity did not vary by more than 10% from its mean value within this disk.

Data acquisition was controlled using custom software written in LabView (National Instruments).

### **Electrophysiology**

Patch clamp experiments were performed at room temperature (25 °C) using an Axopatch 200B amplifier (Molecular Devices). Micropipettes were pulled from borosilicate glass capillary tubes (World Precision Instruments, 1.5 mm OD, 0.84 mm ID) using a dual-stage glass micropipette puller (Narishige, PC-10) to a tip resistance of 5-10 MΩ and filled with intracellular buffer (125 mM potassium gluconate, 8 mM NaCl, 0.6 mM MgCl<sub>2</sub>, 0.1 mM CaCl<sub>2</sub>, 1 mM EGTA, 10 mM HEPES, 4 mM Mg-ATP, and 0.4 mM Na-GTP at pH 7.3; adjusted to 295 mOsm with sucrose). These micropipettes were positioned using a micromanipulator (Sutter Instrument, MP-285). The extracellular solution for all recordings was Tyrode's buffer (125 mM NaCl, 2 mM KCl, 3 mM CaCl<sub>2</sub>, 1 mM MgCl<sub>2</sub>, 10 mM HEPES, and 30 mM glucose at pH 7.3; adjusted to 305–310 mOsm with sucrose). All patch-clamp data were acquired in voltage-clamp mode. Voltage waveforms were generated using a National Instruments DAQ (PCIe-6323) and sent to the Axopatch 200B. Currents were low-pass filtered at 10 kHz by an internal Bessel filter in the Axopatch 200B, and digitized at 50 kHz by the DAQ. Data were analyzed in MATLAB.

### **Preparation of Arch samples from *E. coli***

*E. coli* (strain BL21) were transfected with Archaeorhodopsin-3 in the pET-28b vector under the T7 promoter and grown in LB containing 100 µg/mL kanamycin in a shaking incubator at 37 °C. At an OD<sub>600</sub> of 0.5, protein expression was induced with 0.5 mM IPTG, and 5 µM all-*trans* retinal was added from a concentrated stock in DMSO. Cells were then returned to the incubator and grown for another four hours. Cells were harvested by centrifugation and sonicated on ice for 5 minutes in sonication buffer (150 mM TRIS, 20 mM NaCl, 5 mM MgCl<sub>2</sub>, pH 7.0) using a tip sonicator. The lysate was centrifuged to collect the membranes and the supernatant was discarded. These crudely fractionated membranes were used for most experiments in the microscope. To obtain solubilized protein for transient absorption experiments, sonicated cell membranes were homogenized in a solubilization buffer (30 mM K<sub>2</sub>HPO<sub>4</sub>, 20 mM KH<sub>2</sub>PO<sub>4</sub>, 300 mM NaCl, pH 7.0, 1.5% N-Octyl-β-D-Glucopyranoside) using a glass/Teflon tissue homogenizer, and the mixture was rotated in a Falcon tube (~20 rpm) at 4 °C overnight. The detergent solubilized protein was centrifuged at 13,000 rpm for one hour; the supernatant was stored at 4°C and used for experiments within one week.

### **HEK cell culture**

HEK293T cells were grown in DMEM supplemented with 10% FBS and penicillin/streptomycin in a 37 °C incubator under 5% CO<sub>2</sub>. Cells were grown to 50-70% confluency in 3 cm dishes. 48 hours prior to experimentation, cells were transfected using Transit-293 (Mirus) with a WT Arch-GFP fusion construct under either the CAMKII (Addgene plasmid 22217) or ubiquitin promoter. These cells were trypsinized and re-plated at a density of ~5,000-10,000 cells/cm<sup>2</sup> on matrigel-coated coverglass bottom dishes (P35G-1.5-14-C, MatTek) 12 – 24 hours before experimentation. Although there is some retinal present in FBS, we added all-*trans* retinal (5 µM) to each dish 1 - 2 hours prior to imaging.

## Measuring fluorescence vs. voltage

We measured Arch fluorescence as a function of membrane voltage (Fig. 2a) on HEK cells under whole-cell voltage clamp. The control voltage was a triangle wave between -150 mV and +150 mV, for 10 cycles at a sweep rate of 200 mV/s. The sweep rate was sufficiently slow that no electrical compensation was needed. We recorded fluorescence on a camera and took the average signal from a patch of membrane selected to avoid fluorescence from Arch molecules that had not trafficked to the membrane. We also subtracted background fluorescence from the coverglass and the medium by recording the same signal from a cell-free area of the dish.

The fit to a Hill curve in Figure 2a is based on a model of thermal equilibrium between two states whose energies are separated by  $\alpha(V - V_0)$ . The fluorescence is:

$$F = F_1 + \frac{F_2 - F_1}{1 + e^{\frac{\alpha(V - V_0)}{kT}}} \quad [S1]$$

Where  $F_1$  and  $F_2$  represent the fluorescence produced by each state and  $\alpha V_0$  is the difference in the states' energies in the absence of applied voltage. We fitted Eq. S1 to our data on  $F$  vs.  $V$ , subject to the constraint that  $F_1$  and  $F_2$  must be positive, yielding  $\alpha = 0.15$  and  $V_0 = -280$  mV. Allowing a 1% rms error gives bounds  $0.09 < \alpha < 0.35$  and  $-330 < V_0 < -50$  mV.

## Measuring fluorescence response to a step in voltage

The response of Arch fluorescence to a step in voltage (Fig. 2b) was measured on HEK cells under whole-cell voltage clamp. We applied a square wave between -70 mV and +30 mV at 50 Hz, and collected the fluorescence on a PMT. The output of the PMT passed through an 8-pole Bessel filter with a cutoff of 25 kHz and was digitized at 50 kHz. The graph shows the response averaged for 1 min. Illumination was at 594 nm, 1000 W/cm<sup>2</sup>.

A challenge in measuring fast step responses is that the membrane voltage,  $V_m$  lagged the voltage applied to the patch pipette,  $V_p$ . The capacitance of the cell membrane,  $C$ , and the series resistance of the pipette,  $R_p$ , combined to act as a low-pass filter ( $R_p C \approx 0.5$  ms) on  $V_p$ . This filtering masked the true response speed of Arch. A common resolution to this problem is to use the 'compensation' circuitry in the patch clamp amplifier. The values of  $C$  and  $R_p$  are determined by observing the current produced in response to a step in  $V_p$ . The amplifier then generates a voltage waveform that exaggerates high frequency components of the desired signal to counteract the low-pass filtering of the cell.

Electrical compensation introduces some artifacts, however, because it neglects additional capacitances and resistances that lead to a more complex impulse response than can be accommodated by a simple  $RC$  filter. Additionally, to avoid instabilities in the amplifier, the compensation must be kept below 100%. We thus measured the step response without compensation, as shown in Figure 2b.

We modeled the response of membrane voltage  $V_m$  to a step in  $V_p$  as an exponential with time constant  $\tau_V$ . This time constant was found from the relaxation time of the current in response to a step in  $V_p$ . In the experiment of Fig. 2b,  $\tau_V = 0.4$  ms. We modeled the fluorescence response of

Arch to a step in  $V_m$  as an exponential with time constant  $\tau_F$ . The response of Arch fluorescence,  $F$ , expressed as a fraction of its maximum response, to a step in  $V_p$  is:

$$\begin{aligned}
 F(t) &= \frac{1}{\tau_F} \int_0^t \left(1 - e^{-\frac{t'}{\tau_V}}\right) e^{-\frac{(t-t')}{\tau_F}} dt' \\
 &= 1 + e^{-\frac{t}{\tau_F}} \left(\frac{\tau_V}{\tau_V - \tau_F} - 1\right) - e^{-\frac{t}{\tau_V}} \frac{\tau_V}{\tau_V - \tau_F}
 \end{aligned}
 \tag{S2}$$

Fitting the fluorescence to equation S2 with the single fitting parameter  $\tau_F$ , we find  $\tau_F = 0.4$  ms for a step up in voltage and  $\tau_F = 0.6$  ms for a step down.

Fig. S3 shows the fluorescence step response measured using the capacitance compensation circuitry in the patch clamp amplifier. The bounce in fluorescence is an artifact of the compensation circuitry. This data also shows a time constant of 0.6 ms.

### Measuring fluorescence vs. intensity

The dependence of Arch fluorescence on illumination intensity (Fig. 2c), was measured in a sample of crudely fractionated *E. coli* membranes containing Arch-eGFP. We varied the illumination intensity continuously using an AOTF. We monitored the laser power on a photodiode and the fluorescence on a PMT. Each measurement was repeated twice on the same sample region to check for sample degradation. To check for nonlinearities in the response of the photodiode or the PMT we performed the same experiment on a sample of fluorescent beads (Invitrogen). We placed neutral density filters on the excitation and emission paths to ensure that the PMT and photodiode were operating in the same range as they were during the Arch experiment. We found no nonlinearities in the electronics or detectors.

We determined the relative brightness of Arch and eGFP in a 1:1 Arch-eGFP fusion. eGFP was excited at 488 nm and emission was passed through a 531/40 bandpass filter. Arch emission was passed through a 710/100 bandpass filter. In both cases the fluorescence was collected on a PMT. The data was corrected for the wavelength dependence of the PMT quantum efficiency, which was nearly twice as high at 531 nm as at 710 nm.

### Imaging sequential multiphoton excitation of Arch fluorescence in a cuvette

Figure 2d demonstrates the multiphoton character of Arch fluorescence. The data was taken in a cuvette containing detergent-solubilized Arch-eGFP. Illumination was provided by two lasers: 473 nm to excite eGFP, 594 nm to excite Arch. To ensure that the beam shape parameters were identical for both channels, the beams were expanded and then cropped by an iris at the back of the objective (Olympus, 20× NA 0.4). The image was taken using a photographic lens (Nikon, 60 mm f/2.8) and an Andor EMCCD camera (iXon3 897). The image is a composite of a white light image of the cuvette (no emission filter) mapped to the white channel, an image of Arch fluorescence (710/100 emission filter, 594 excitation, 500 1 second exposures averaged) mapped to a red channel, and an image of eGFP fluorescence (531/40 emission filter, 473 nm excitation, 60 1 s exposures averaged) mapped to a green channel.

## Action spectra

The action spectra of Arch, (Fig. 2e), were collected as follows:

1. Fluorescence and voltage sensitivity spectra were obtained from HEK cells ( $n = 4$ ) expressing Arch. Membrane voltage was controlled by whole-cell patch clamp. Cells were illuminated with light from a supercontinuum laser at eight evenly-spaced wavelengths between 530 nm and 635 nm (set by an AOTF), at  $I = 10 \text{ W/cm}^2$ . The AOTF was calibrated with a power meter to ensure that intensity did not change across wavelengths. Each cell was illuminated for 5 s at each wavelength while the voltage cycled through the values, in mV: 0, -100, 0, +100, 0, spending 1 s at each voltage. Fluorescence was recorded on an EMCCD, and the 150 most voltage-responsive pixels (corresponding to membrane-localized Arch) were selected for analysis using the weighting algorithm described previously (1).

The fluorescence excitation spectrum was determined from the mean fluorescence at each wavelength. The voltage sensitivity spectrum was determined from the difference between the fluorescence excitation spectrum at +100 mV and the spectrum at -100 mV.

2. The absorption spectrum was acquired on detergent-solubilized Arch (in solubilization buffer at pH 7.0) using a Nanodrop 2000c (Thermo Scientific) (Fig. S5). The path length was 1 cm. To determine the absolute extinction coefficient of Arch we extracted the retinal using a method based on that of El Sayed et al. (2). Briefly, an aliquot of detergent-solubilized Arch was diluted 4x in a 2:1 chloroform:methanol solution. Retinal was cleaved from the protein by adding 20  $\mu\text{L}$  of 1 M hydroxylamine. The resulting retinal oxime was collected in the chloroform fraction by shaking the sample for ~5 minutes. An absorption spectrum of the chloroform showed a peak at 362 nm, corresponding to free retinal oxime (Fig. S5). Using the extinction coefficient of retinal oxime ( $60,000 \text{ M}^{-1}\text{cm}^{-1}$ ), we calculated the concentration of extracted retinal oxime.

We then repeated the chloroform extraction on a sample of free retinal of known concentration (25  $\mu\text{M}$ ) in solubilization buffer, and measured the absorption spectrum of the extracted retinal (Fig. S5). Using the extinction coefficient of *all-trans* retinal ( $43,000 \text{ M}^{-1}\text{cm}^{-1}$ ), we calculated that our extraction efficiency was ~58%. Assuming a 1:1 stoichiometry of retinal binding by Arch and an extraction efficiency of 58% for retinal oxime, we determined the concentration of the original Arch sample and used this to calculate the extinction coefficient of Arch at 552 nm ( $\epsilon = 50,300 \text{ M}^{-1}\text{cm}^{-1}$ ).

3. The photocurrent action spectrum was obtained from a HEK cell expressing Arch. The membrane voltage was clamped at 0 V via whole-cell patch clamp. The cell was illuminated with light from a supercontinuum laser at eight evenly-spaced wavelengths between 530 nm and 635 nm (set by an AOTF), at  $I = 10 \text{ W/cm}^2$ . Exposures (1 s) alternated with darkness (1 s). The difference in membrane current between these conditions yielded the photocurrent action spectrum.

## Transient absorption

Transient absorption experiments (Fig. 3a, b; Fig. 4c) were performed on a home-built apparatus. Detergent-solubilized Arch at pH 6, 7, or 8 was held in a quartz cuvette. Excitation was provided by a frequency-doubled Nd:YAG laser (Spectraphysics INDI-40) producing 5 ns pulses at 532

nm, with a 20 Hz repetition rate. We used an optical chopper to block every second pulse, so the sample saw flashes every 100 ms. White light from a 100 W Hg arc lamp (Olympus) passed through a motorized monochromator (Horiba Scientific, iHR320) then through the cuvette. The transmitted light was recorded on a photodiode (Thorlabs, DET36A) and digitized at 100 kHz on a National Instruments DAQ (PCIe-6259). We recorded for 5 s (50 pump cycles) at each wavelength, and cycled through the wavelengths 20 times.

We recorded absorption for every pump pulse, only averaging in post-processing, so that we could check for degradation of the sample. We saw some bleaching of the sample but the shape of the spectra did not change with time. We also recorded the photodiode signal with each of the beams (pump and probe) independently shuttered to check for electrical artifacts. We varied the pump intensity to ensure that the signal was linear in pump intensity.

### Fitting transient absorption data

We fit the transient absorption data in Fig. 2b to exponential curves of the form

$$I(\lambda, t) = \sum_{i=1}^n B_i(\lambda) e^{\frac{-t}{\tau_i}} \quad [S2]$$

At 400 nm and 560 nm, the absorption vs. time traces were fit to this equation with  $n = 3$  to determine the rates (“ $\tau$ ”) and weights (“ $B$ ”) shown in Table S1. The first two time constants from this fit were held as fixed parameters when fitting the absorption vs. time at 640 nm to an equation of the same form (with  $n = 4$ ,  $\tau_1 = .04$  ms, and  $\tau_2 = .39$  ms). The rates and weights from this fit are shown in Table S1. The fits to the data at all three wavelengths are plotted as black lines in Figure 3b.

	$\tau_1 = .04$ ms	$\tau_2 = .39$ ms	$\tau_3 = 4.1$ ms	$\tau_4 = 14.3$ ms	$\tau_5 > 100$ ms
400 nm	-1.7	4.8	<i>n/a</i>	<i>n/a</i>	.5
560 nm	1.7	-5.3	<i>n/a</i>	<i>n/a</i>	-3.9
640 nm	.30	-.34	-.65	.90	<i>n/a</i>

Table 1. Weights ( $B_i \times 10^3$ ) of indicated components from fitting transient absorbance data in Figure 2b to Eq. S2 with  $n = 3$  (400 nm, 560 nm) or  $n = 4$  (640 nm).

### Transient fluorescence

Transient fluorescence measurements (Fig. 3c) were performed on crudely fractionated *E. coli* membranes containing Arch, in our home-built microscope. Pump pulses were 532 nm, 50 W/cm<sup>2</sup>, and lasted 100  $\mu$ s. To minimize the perturbation due to the probe, we used dim red probe pulses (640 nm, 15 W/cm<sup>2</sup>), and only recorded fluorescence during the first 20  $\mu$ s of the probe pulse. We verified that the fluorescence signal was linear in probe intensity. We waited 150 ms between pump pulses. Waiting longer did not affect the data.

Each data point represents the average of 30 pump-probe cycles. PMT and photodiode signals were filtered at 50 kHz and digitized at 100 kHz. The raw data traces showed negligible sample degradation during these experiments.

The triple pulse (pump-pump-probe) scheme provides rich information on light-driven transitions of photocycle intermediates, and the lifetimes of the resulting states. In addition to the data shown in Fig. 3c we varied the intervals between pulses (Figure S9), the wavelength of each pump (Figure S10) and the intensity of each pump (Figure S11).

### Confocal scan

Figure 3e shows four images taken on a commercial scanning confocal microscope (Zeiss LSM 710) of a HEK293T cell expressing an Arch-eGFP fusion. Arch was excited at 594 nm and eGFP was excited at 488 nm. The scan rate was 0.47 ms per line. The ‘line scan’ mode scanned each line 16 times before moving on to the next line whereas the ‘frame scan’ mode scanned the entire field of view, line-by-line, and repeated 16 times.

### Time- and voltage-dependent fluorescence in HEK cells

Time-dependent fluorescence and photocurrent (Fig. 4a, b, d) were measured in single HEK cells expressing Arch under whole-cell voltage clamp.

To investigate the fluorescence response to onset of illumination at different voltages (Fig. 4a), the membrane potential was set to -100 mV or +100 mV via whole cell patch clamp. The cell was exposed to a pulse of light (50 ms, 594 nm, 1000 W/cm<sup>2</sup>) followed by 250 ms of darkness and the fluorescence was recorded (Fig. 4a). The cycle was repeated 10 times. Average fluorescence responses show that fluorescence and voltage sensitivity arose several milliseconds after onset of continuous illumination.

To investigate the fluorescence response to a brief flash of light (Fig 4b, F and  $\Delta F$ ), we initiated the photocycle with a flash (1000 W/cm<sup>2</sup>, 100  $\mu$ s, 594 nm), and then probed the fluorescence with a second flash (1000 W/cm<sup>2</sup>, 100  $\mu$ s, 594 nm) with variable delay,  $t$ . Each data point is the average of 80 pump-probe measurements. To measure F, the membrane voltage was clamped at  $V_m = 0$ . To measure  $\Delta F$ , the membrane voltage was held fixed at +30 mV and then at -70 mV.

The probe flashes were sufficiently intense to drive  $N \rightarrow Q$  and to excite fluorescence of  $Q$ , i.e. to provide photons 2 and 3 in the scheme of Fig. 3d. Intense probe beams were necessary for the single-cell measurements due to the much smaller sample volume compared to the experiments on fractionated *E. coli* membranes. The fluorescence measured at the single-cell level peaked at  $t = 5$  ms, similar to that measured in bulk (Fig. 3c(iii)). Considering the different protein environments (crudely fractionated *E. coli* membranes vs. intact HEK cells), we do not consider the difference in timing to be significant.

To investigate the effect of violet flashes on steady-state fluorescence and photocurrent at different voltages (Fig. 4d, S13), the membrane potential was varied in steps of 30 mV from -90 mV to +60 mV. At each voltage, pulses of red light were applied to elicit steady-state fluorescence and photocurrent (100 ms, 640 nm, 4000 W/cm<sup>2</sup>). 54 ms after turning on the red light, a short pulse of violet light (11 ms, 407 nm, 40 W/cm<sup>2</sup>) was applied to the cell to perturb steady-state fluorescence and photocurrent. The red light was turned off for 100 ms between red pulses. This procedure was repeated four times at each voltage. Background fluorescence due to the 407 nm light alone was subtracted from fluorescence measurements.

## Ground-state recovery probed by two-pulse photocurrent

The integrated photocurrent following a brief pulse of light provides a measure of the ground state population of Arch. By measuring this photocurrent under a two-pump protocol with variable delay, we probed the duration of the photocycle.

HEK cells expressing Arch were held at a membrane voltage of 0 mV via whole cell patch clamp. Cells were exposed to two flashes of light (100  $\mu$ s, 594 nm, 1000 W/cm<sup>2</sup>) with variable delay,  $t_{\text{probe}}$ . Membrane current was recorded continuously. The protocol was repeated at 600 ms intervals.

## Transient capacitance measurements

A voltage-dependent equilibrium between differently charged states should manifest as an increase in membrane capacitance. If this equilibrium only occurs at a certain time in the photocycle, then one expects to detect a time-dependent capacitance subsequent to a flash of light. To measure time-dependent capacitance (Fig. 4b), we set  $V_m = V_0 + A\sin(2\pi ft)$ , with  $V_0 = -25$  mV,  $A = 35$  mV and  $f = 1$  kHz. We recorded the current while flashing light every 400 ms (100  $\mu$ s flashes, 532 nm, 500 W/cm<sup>2</sup>).

Here we discuss how to calculate this time-dependent capacitance from time-resolved AC electrical impedance measurements. We modeled the cell by the circuit shown in Figure S14, consisting of the pipette resistance,  $R_p$  ( $\approx 20$  M $\Omega$ ), the membrane resistance,  $R_m$  ( $\approx 500$  M $\Omega$ ), and the membrane capacitance,  $C$  ( $\approx 20$  pF). We applied a 1 kHz AC voltage  $V(t) = \text{Re}(Ve^{i\omega t})$  and recorded the current.

Allowing for time-dependent capacitance, the dynamics of the circuit are described by

$$i = \frac{V_m}{R_m} + \frac{dV_m}{dt}C + V_m \frac{dC}{dt} \quad [\text{S3a}]$$

$$i = \frac{V-V_m}{R_p} \quad [\text{S3b}]$$

where  $V_m$  is the voltage across the membrane. Eq. S3a has an important difference from the usual description of time-dependent current in an electric circuit. Usually, the relation  $Q = CV$  leads to the time-dependent expression  $i = C \frac{dV}{dt}$ . However, in a circuit where the capacitance may change on the same timescale as the voltage, one must include an additional contribution to the current,  $V \frac{dC}{dt}$ .

We made two simplifying assumptions: 1) the membrane resistance was large compared to the impedance of the membrane capacitance ( $R_m \gg 1/(\omega C)$ ) and 2) the capacitance changed slowly relative to the frequency of the applied voltage. This second approximation is almost certainly not true early in the photocycle, but is likely to be true on timescales long compared to the period of the probe voltage (1 ms in the present experiment), because molecular dephasing suppresses the effects of fast transitions late in the photocycle. With these approximations, we can ignore the term  $V_m \dot{C}$  and estimate  $C(t)$  as:



$$C(t) = \frac{-1}{\omega \text{Im}[\tilde{V}(t)/\tilde{I}(t)]} \quad [\text{S4}]$$

In Eq. S4,  $\tilde{V}(t)$  and  $\tilde{I}(t)$  are the Fourier components of voltage and current at the driving frequency, defined with the Fourier integral performed over a single period,  $\Delta t$ .

$$\tilde{V}(t) = \int_{t-\Delta t/2}^{t+\Delta t/2} e^{-i\omega t'} V(t') dt',$$

and similarly for  $\tilde{I}(t)$ .

### Interpretation of transient capacitance

Here we relate transient capacitance to molecular parameters using a simple model. Consider an equilibrium between two states of Arch whose substantial difference is the position of a single charge (a proton, say) as shown in Figure S14. A voltage  $V_m$  applied to the membrane shifts the relative energies by an amount  $V_{eff} = \alpha(V_m - V_0)$ , where  $\alpha$  represents the fraction of total membrane voltage drop that occurs between the two possible charge locations.  $V_0$  is the membrane voltage at which the states have equal energy. The probability of populating state 1, in terms of the effective voltage  $V_{eff}$ , is given by the Boltzmann distribution:

$$p = \frac{1}{1 + e^{\frac{-eV_{eff}}{kT}}}$$

This system acts as a capacitor in that the distribution of charges is a function of voltage. Near  $V_{eff} = 0$ , the capacitance is given by:

$$C = \frac{dQ}{dV_{eff}} = e \frac{dp}{dV_{eff}} = \frac{e^2}{4kT} = 1.6 \times 10^{-18} \text{ F}. \quad [\text{S5}]$$

How does this capacitance affect the capacitance of the membrane? The charge is capacitively coupled to the conducting regions on either side of the membrane as shown in Figure S14. The contribution to the total capacitance will depend on  $\alpha$ , the fraction of the membrane voltage drop which occurs between the two charge locations. This fraction must also be the ratio of the two capacitances  $C_1$  and  $C_2$  shown in Figure S14. The contribution of the voltage-dependent equilibrium of a single Arch molecule to the total membrane capacitance is therefore:

$$\Delta C = \alpha^2 \frac{e^2}{4kT}. \quad [\text{S6}]$$

Our measurement of transient capacitance yielded  $\Delta C/N = 1.7 \times 10^{-20} \text{ F}$ , where  $N$  is the number of molecules of Arch in the membrane, determined by transient photocurrent (see below). These results give  $\alpha = 0.1$ . This measurement is in fair agreement with the estimate  $0.09 < \alpha < 0.35$  determined by fitting a Hill curve to our fluorescence versus voltage data, especially considering the very different nature of these two measurements.

### Estimate of density of Arch molecules

We obtained an estimate of the areal density of Arch molecules by considering the photocurrent following a pulse of light. The integrated charge displacement after a pulse of 50 W/cm<sup>2</sup> for 100 μs was 1.1 pC, or 7×10<sup>6</sup> protons. Based on the photocurrent saturation curve (Fig S4) we estimate 50% activation of Arch under these illumination conditions. We thus estimated the total number of Arch molecules in the plasma membrane to be  $N = 1.4 \times 10^7$ . For the same cell, the capacitance measurement described above yielded a membrane capacitance of 41 pF. Assuming a membrane capacitance of 1 μF/cm<sup>2</sup>, gives approximately 3500 Arch molecules per square micron.

### Model of voltage-dependent fluorescence in Arch

We modeled the photocycle of Figure 2e quantitatively. We assigned rates to each transition in this model:  $k_{GM}$  = ground to  $M$  under red illumination (with no red light,  $k_{GM} = 0$ );  $k_{NG}$  =  $N$  to ground;  $k_{MG}$  =  $M$  to ground under violet illumination (with no violet light,  $k_{MG} = 0$ ). We assigned fractional charge movements to each forward transition in the model ( $Q_{GM}$  and  $Q_{NG}$ ) such that the total charge moved in the photocycle is 1 ( $Q_{GM} + Q_{NG} = 1$ ), and we assumed that the charge movement from ground to  $M$  is equal and opposite to the charge movement from  $M$  to ground ( $Q_{GM} + Q_{MG} = 0$ ). We assumed that  $M$  and  $N$  equilibrate quickly to an equilibrium given by  $K(V)$  satisfying a two-state Boltzmann distribution:

$$K(V) = e^{\frac{\alpha(V-V_0)}{k_B T}}$$

We further assumed that fluorescence was proportional to the population of  $N$ , with proportionality constant  $F_1$  allowing for a small constant background fluorescence,  $F_0$ . The populations evolve according to:

$$M = N/K$$

$$\frac{d}{dt} \begin{bmatrix} G \\ N \end{bmatrix} = \begin{bmatrix} -k_{GM} & k_{NG} + k_{MG}/K \\ k_{GM}K/(K+1) & -k_{NG}K/(K+1) - k_{MG}/(K+1) \end{bmatrix} \begin{bmatrix} G \\ N \end{bmatrix}$$

while the fluorescence  $F$  and current  $I$  are given in terms of the states' populations:

$$F = F_0 + F_1 N$$

$$I = I_1(Q_{GM}k_{GM}G - Q_{GM}k_{MG}M + Q_{NG}k_{NG}N)$$

where  $I_1$  is the constant of proportionality equal to the number of molecules in the membrane.

We solved for the  $N$  population after the onset of illumination:

$$N(t) = \frac{\left(1 - e^{-\frac{(k_{MG} + k_{GM} + K(k_{NG} + k_{GM}))t}{1+K}}\right) K k_{GM}}{k_{MG} + k_{GM} + K(k_{NG} + k_{GM})}$$

which reduces to the following under steady-state illumination ( $t = \infty$ ):

$$N = \frac{Kk_{GM}}{k_{MG} + k_{GM} + K(k_{NG} + k_{GM})}$$

Fluorescence and current were calculated using the equations given above under both steady-state illumination and as a function of time after the onset of red illumination ( $k_{MG} = 0$ ). This model was able to reproduce the main features of the data shown in Figure 4(d) using the following parameters:  $k_{GM} = .5 \text{ ms}^{-1}$ ,  $k_{NG} = .033 \text{ ms}^{-1}$ ,  $k_{MG} = .2 \text{ ms}^{-1}$ ,  $Q_{GM} = 0.09$ ,  $\alpha = 0.35$ , and  $V_0 = -30 \text{ mV}$ . The fits resulting from using these parameters are shown in Fig. S13.

## Supplementary Figures

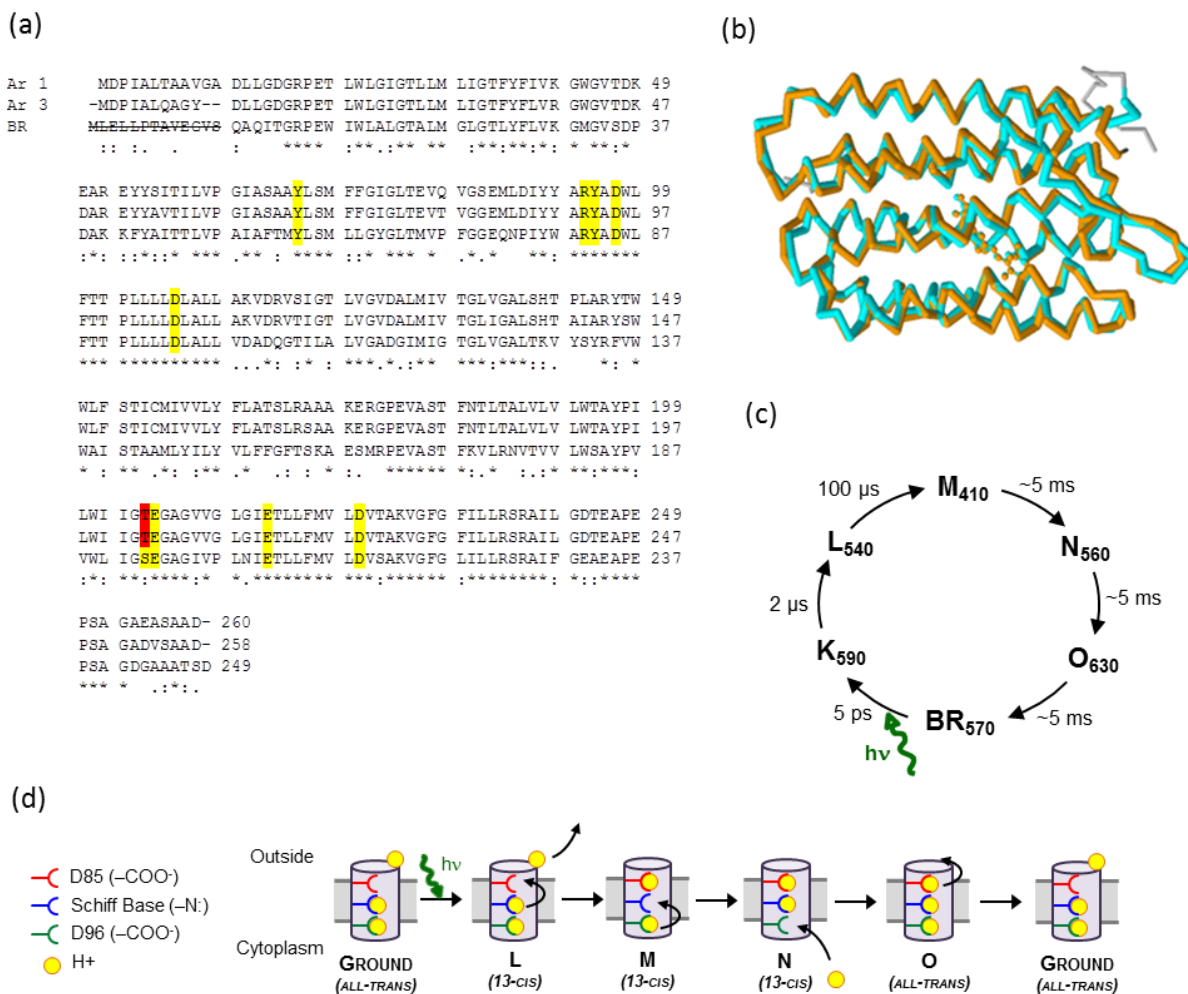


**Figure S1. Comparison of Arch-3, Arch-1, and Bacteriorhodopsin.** (a) Sequence alignment via ClustalW2. Arch-1 (Uniprot P69051) and Arch-3 (Uniprot P96787) share 93% amino acid identity. Arch-3 and BR share 61% amino acid identity. All key residues in the proton-pumping pathway (yellow) are shared except for S193 in BR (T203 in Arch-3). This residue is part of the extracellular proton release group. The first 13 amino acids of BR are removed in a posttranslational modification. BR residue numbering has been adjusted to reflect spectroscopic convention. (b) Structural alignment of Arch-1 (pdb 1UAZ) (3) with BR (pdb 1FBB) by jFATCAT. No structural adjustment was allowed. The RMSD between the structures was 1.07 Å. (c) Simplified version of the BR photocycle with absorption maxima of each state, adapted from (4). (d) Simplified cartoon of one cycle of the BR photocycle (omitting the short-lived K state and ignoring back-reactions and branches) showing how a proton moves from the cytoplasmic side to the extracellular side. In BR, D85 is the proton acceptor, and D96 is the proton donor. These residues correspond to D95 and D106, respectively, in Arch-3.

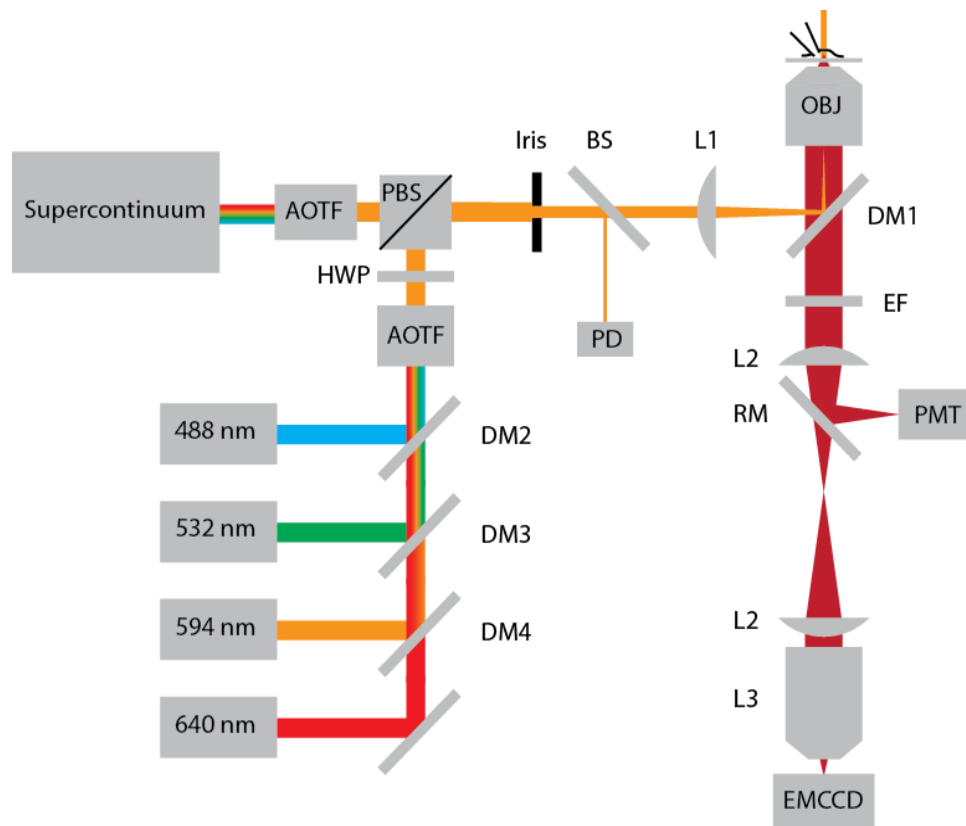


**Figure S2. Schematic diagram of home-built microscope.** AOTF: acousto-optic tunable filter. EMCCD: electron-multiplying charged-coupled device camera. PMT: photomultiplier tube. OBJ: Objective lens. EF: emission filter. DM(1-4): dichroic mirror. PBS: polarizing beam splitter. HWP: half-wave plate. PD: photodiode. BS: beam splitter. L1, L2 achromatic lenses. L3: photographic lens. RM: removeable mirror.

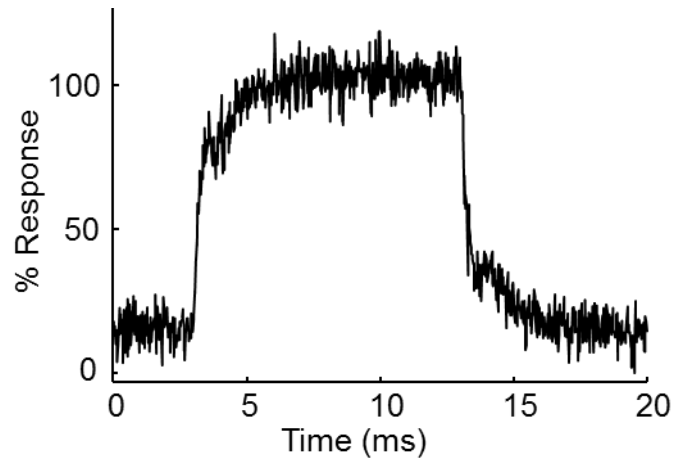


**Figure S3. Compensated fluorescence step response.** Fluorescence response to a step in voltage between  $-70$  mV and  $+30$  mV similar to that shown in Figure 2b, but with patch-clamp amplifier compensation circuitry enabled. The initial fluorescence response reflects the intrinsic response time of Arch. The bounce in fluorescence is an artifact of the compensation circuitry.

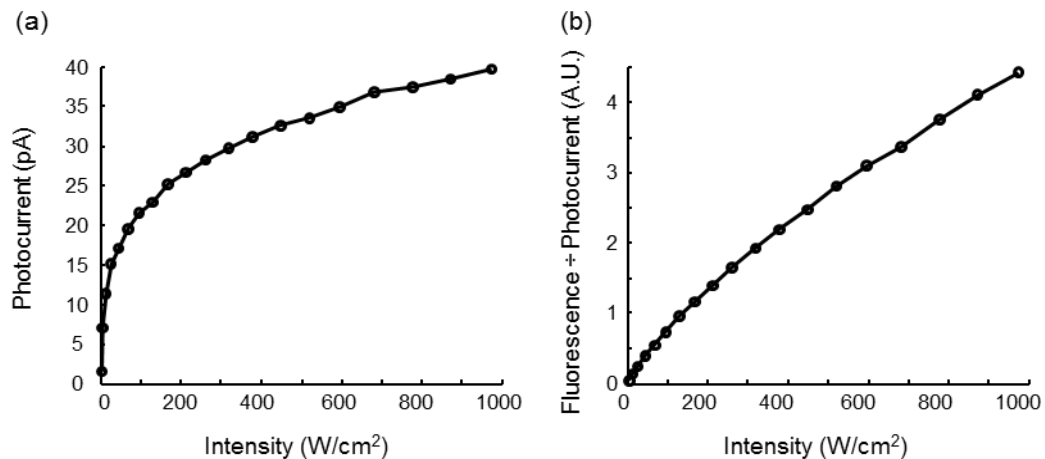


**Figure S4. Saturation of Arch photocurrent at 594 nm.** (a) Steady-state photocurrent in a HEK cell expressing Arch, as a function of illumination intensity at 594 nm. Membrane voltage was held at 0 mV by whole-cell patch clamp. The cell was alternately exposed to 50 ms of illumination and 50 ms of darkness. The plot shows the average difference in membrane current between these conditions. Each data point represents the average of 6 measurements. (b) Fluorescence per pA of photocurrent, recorded on the same cell as in (a). At higher illumination intensity, the fluorescence signal grew superlinearly, while the photocurrent saturated. Thus fluorescence measurements yield maximum signal relative to perturbation to membrane potential when the illumination was concentrated on a small piece of a cell. If fluorescence and photocurrent were both linear in illumination intensity, the graph in (b) would be a horizontal line.

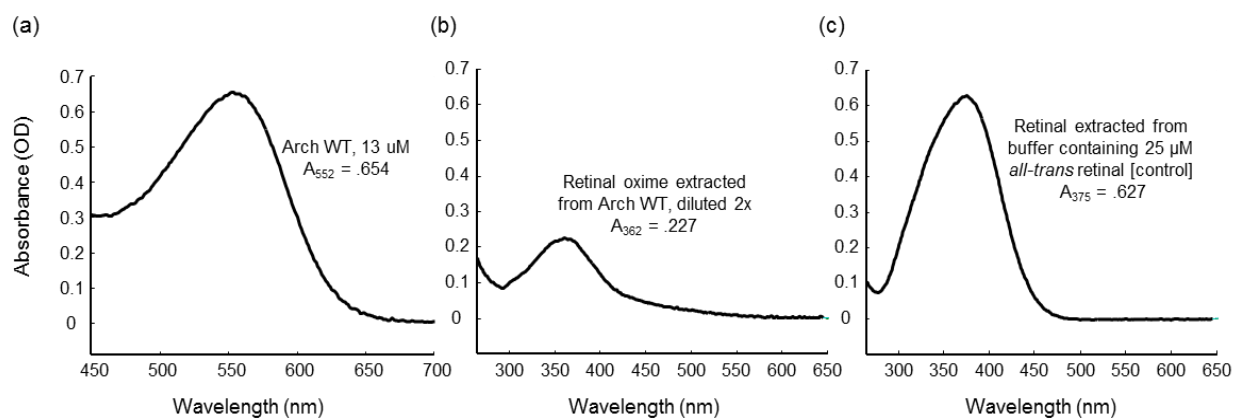


**Figure S5. Determination of the extinction coefficient of Arch.** (a) Absorption spectrum of detergent-solubilized Arch, pH 7 (b) Absorption spectra of retinal oxime extracted from the sample in (a). (c) Absorption spectrum of retinal extracted from a reference sample of known concentration.



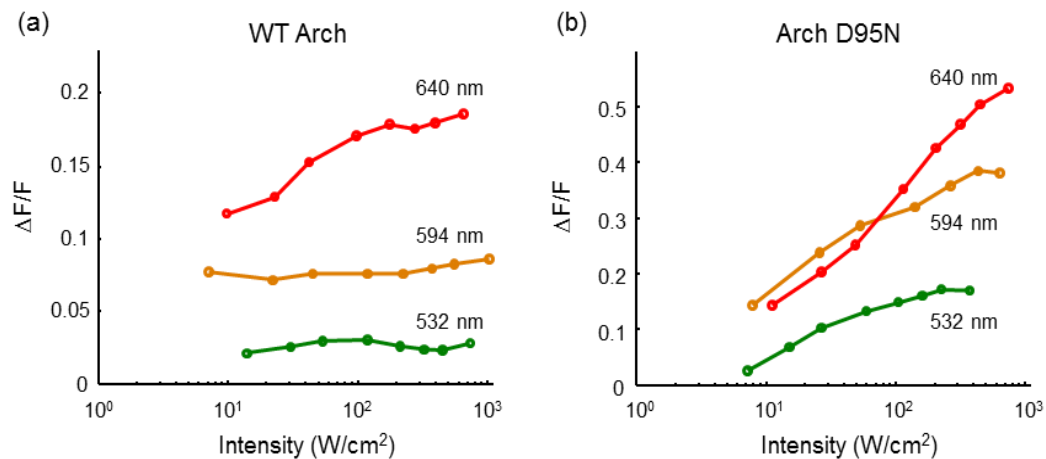


**Figure S6. Voltage sensitivity vs. illumination intensity for Arch and Arch(D95N).** (a) Voltage sensitivity ( $\Delta F/F$ ) of Arch WT increased nearly two-fold between  $10 \text{ W/cm}^2$  and  $650 \text{ W/cm}^2$  under illumination at  $640 \text{ nm}$ , while voltage sensitivity was independent of illumination intensity under illumination at  $532 \text{ nm}$  and  $594 \text{ nm}$ . Note that the parameter plotted here,  $\Delta F/F$ , is different from the absolute change in fluorescence,  $\Delta F$ , which is plotted in Figure 2e. (b) In contrast, the voltage sensitivity of Arch D95N increased markedly with illumination intensity at all three wavelengths. Sensitivity increased 5x between  $10 \text{ W/cm}^2$  and  $700 \text{ W/cm}^2$  at  $640 \text{ nm}$ . These results imply that fluorescence of Arch WT is dominated by a single fluorescent species, with possibly a weak contribution from a red-shifted voltage-insensitive state. Fluorescence of Arch(D95N) appears to have contributions from voltage sensitive and insensitive states, with the photostationary equilibrium shifting toward the voltage sensitive state(s) at higher illumination intensity.

HEK cells expressing Arch WT or Arch(D95N) were subjected to whole-cell voltage clamp and exposed to illumination of specified wavelength and intensity. Fluorescence was recorded on an EMCCD. At each wavelength, intensity was increased in steps (1.6 seconds per step) from 0 to  $\sim 800 \text{ W/cm}^2$ . At each intensity, membrane voltage was stepped between  $-70 \text{ mV}$  and  $+30 \text{ mV}$  four times at a frequency of  $2.5 \text{ Hz}$ . The entire waveform was repeated 2x per cell to ensure stability of the system.  $\Delta F/F$  was calculated as the change in fluorescence over  $100 \text{ mV}$  (between  $-70 \text{ mV}$  and  $+30 \text{ mV}$ ) divided by the fluorescence at  $-70 \text{ mV}$  of the 150 most responsive pixels (as determined using the weighting algorithm outlined by Kralj *et al.* (1)). In (a) and (b) data is averaged over  $n = 2$  cells.

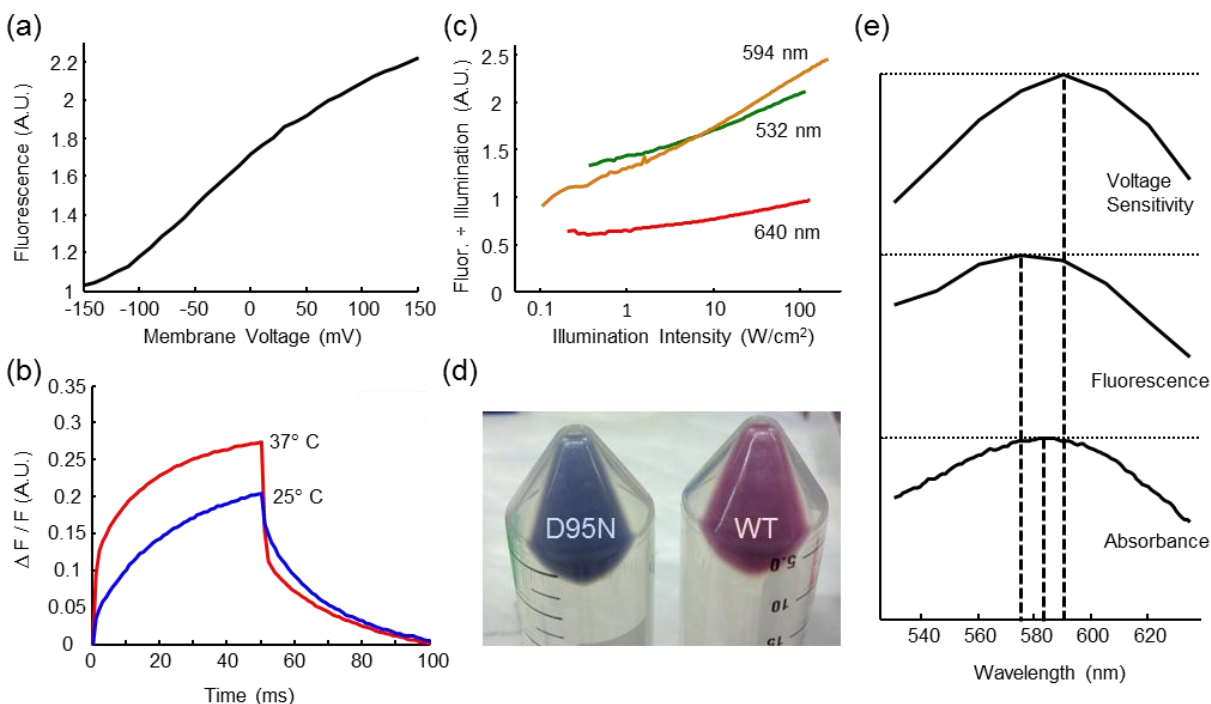


**Figure S7. Characterizing Arch(D95N).** (a) Voltage-sensitive fluorescence of Arch(D95N) (exc. 594 nm, 1000 W/cm<sup>2</sup>, em. 660 – 760 nm) in HEK cells at 25 °C. Membrane voltage was controlled via whole-cell patch clamp. Fluorescence was recorded on an EMCCD camera. (b) Fluorescence response to a voltage step between -80 mV and +20 mV at two temperatures. (c) Ratio of fluorescence to illumination intensity ( $F/I$ ), as a function of illumination intensity, showing the nonlinear response of Arch(D95N) fluorescence. (d) Picture of *E. coli* expressing Arch(D95N) (left, blue) and Arch (right, purple), demonstrating the difference in ground-state absorption spectra of these two species. (e) Action spectra for Arch(D95N) (analogous to those obtained for WT Arch in Figure 2(e)). Arch(D95N) did not generate a detectable photocurrent.

### Dark adaptation of Arch

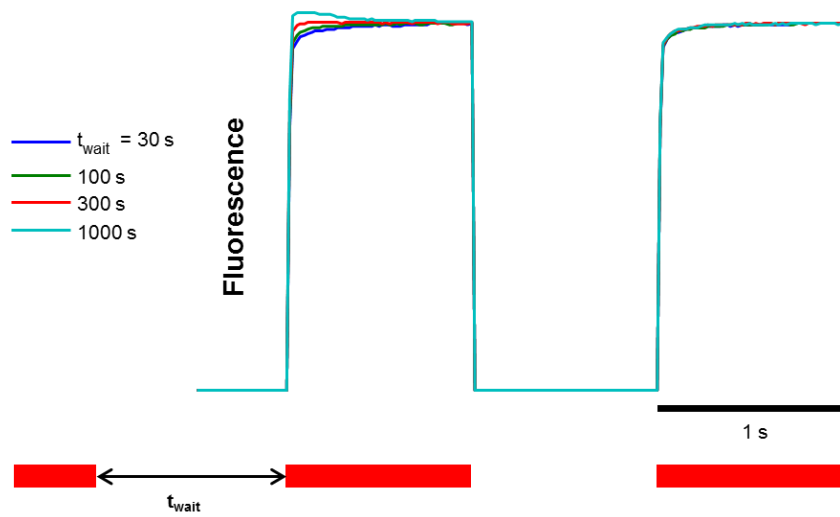


**Figure S8. Dark adaptation of Arch.** Arch was expressed in *E. coli* as described previously and illuminated with two pulses of red light (637 nm, 200 W/cm<sup>2</sup>) as shown. The sample was then left in the dark for some duration  $t_{\text{wait}}$  and the sequence was repeated. The initial fluorescence during the first pulse depended on the time ( $t_{\text{wait}}$ ) since the previous pulse, demonstrating that Arch underwent a very slow ( $\sim 5$  minutes) change in the dark.

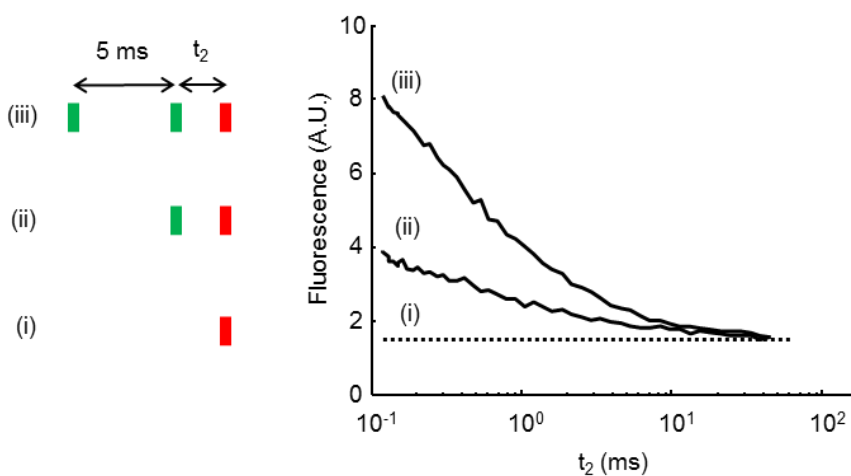


**Figure S9. Nonlinear fluorescence properties of Arch.** Decay of the fluorescent  $Q$  state. Fluorescence was recorded as a function of the delay between the last pump pulse and the probe. Illumination and recording conditions were as in Fig. 3c. Curve (i) shows the low fluorescence of the ground state. Curve (ii) shows that a single pump pulse created a small fluorescent population which decayed in 1.0 ms. Curve (iii) shows the decay of the fluorescent  $Q$  state created by two sequential pump pulses 5 ms apart. The  $Q$  state decayed in 0.84 ms. The similar decay rates in curves (ii) and (iii) led us to conjecture that they reflect the same state, i.e. that there exists a small population in the pre-fluorescent  $N$  state in Arch in the dark.

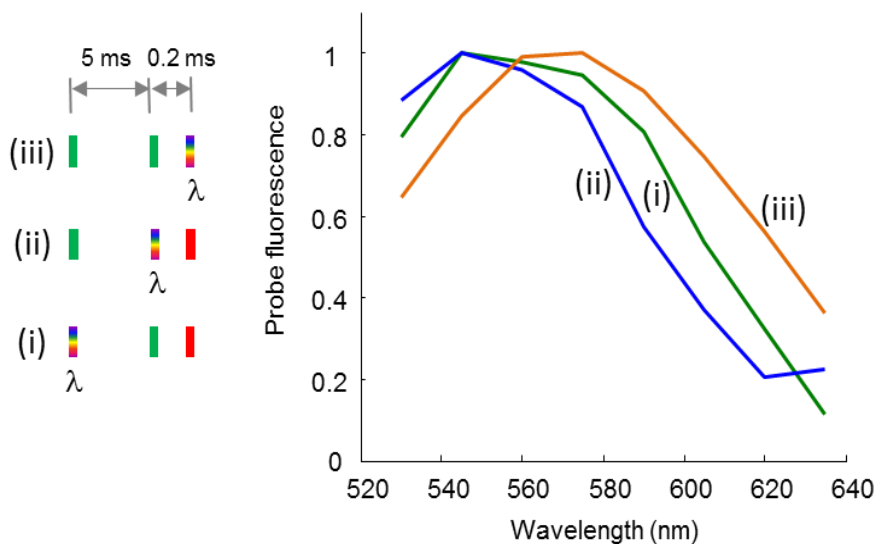


**Figure S10. Action spectra of each photon-mediated transition.** We determined the spectrum of each photon-mediated transition by varying the wavelengths of each illumination pulse while keeping the other pulses fixed. The initial fluorescence elicited by the final pulse is plotted as a function of the wavelength of either the first (i), second (ii), or third (iii) photon.

Illumination and recording conditions were as in Fig. 3c. The variable-wavelength pulses were at an intensity of  $0.7 \text{ W/cm}^2$  and were obtained from the supercontinuum laser. The fixed-wavelength pulses were at  $532 \text{ nm}$ ,  $50 \text{ W/cm}^2$  for pumps 1 and 2, and  $640 \text{ nm}$ ,  $15 \text{ W/cm}^2$  for the probe pulse. All pulses were  $100 \mu\text{s}$  long. Fluorescence was determined from the first  $20 \mu\text{s}$  of the probe pulse to ensure that the probe did not perturb the state of the protein. We verified that fluorescence was linear in the probe intensity.

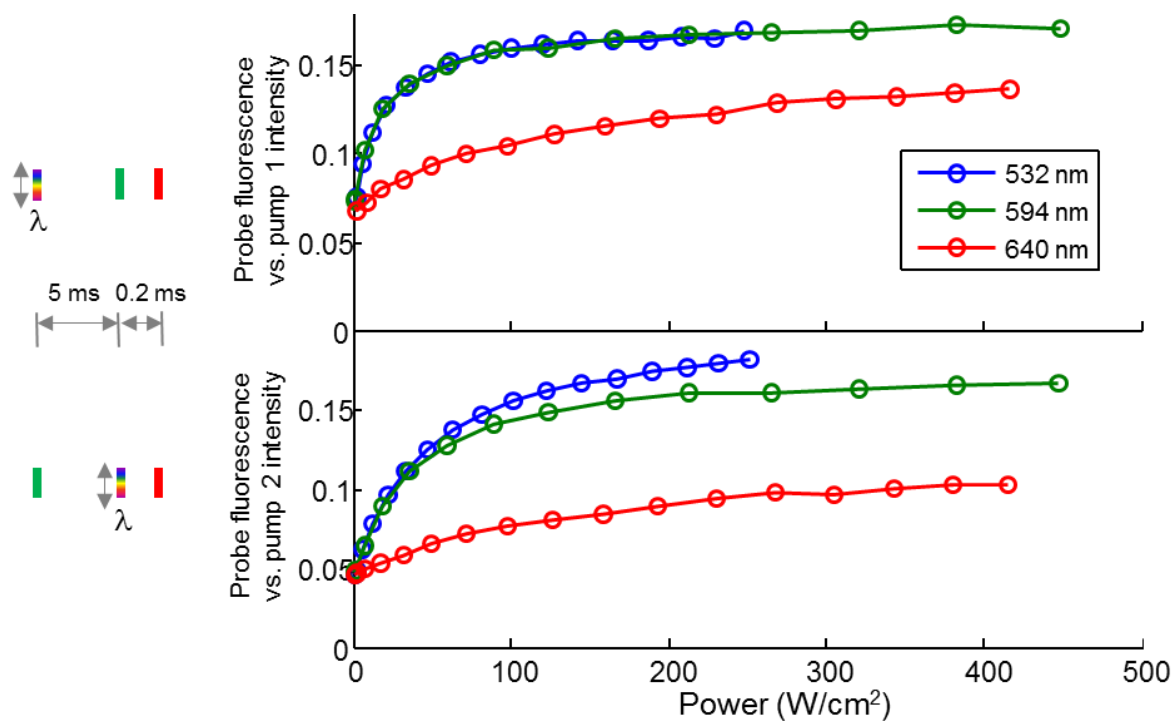


**Figure S11. Saturation of the first two photon-mediated transitions.** We varied the intensity of pumps 1 and 2 to measure the saturation of these optically driven transitions. In all cases the pumps were 100  $\mu\text{s}$  long and the fixed-intensity pump was at 532 nm, 50  $\text{W}/\text{cm}^2$ . When the pump wavelength was 640 nm, the saturation value of the fluorescence was lower than when the pump wavelength was 594 nm or 532 nm. This was true for both the first and second pumps. These results suggest a possible back-reaction or non-pumping shortcut in the photocycle with a red-shifted action spectrum. We did not detect saturation of the third pulse (the pulse responsible for exciting fluorescence). Due to the extremely short excited state lifetime of  $Q$  ( $\sim 62$  ps in BR), this state is expected to saturate at experimentally inaccessible intensities.

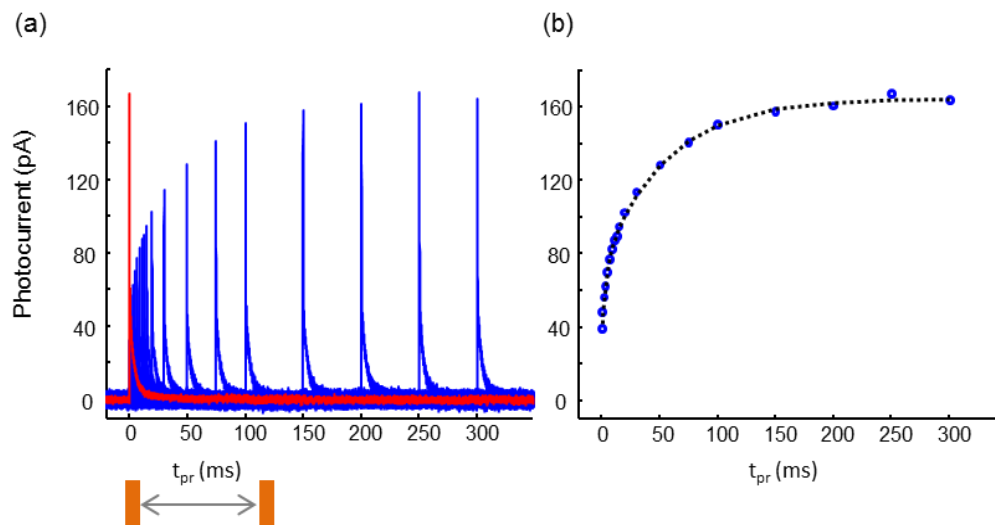


**Figure S12. Ground state recovery measured by photocurrent in HEK cells.** We measured the time-course of ground state recovery in HEK cells by monitoring the photocurrent recovery in a two-pulse experiment. (a) Current due to the first illumination pulse (red). Additional current due to each probe pulse (blue). (b) Peak photocurrents from the second pulse (blue circles). Fit to a double exponential (black dotted line) with time constants of 3.8 ms (weighting coefficient = 1) and 54 ms (weighting coefficient = 3). When photocurrent recovery was fit to a single exponential, the time constant was 32 ms.

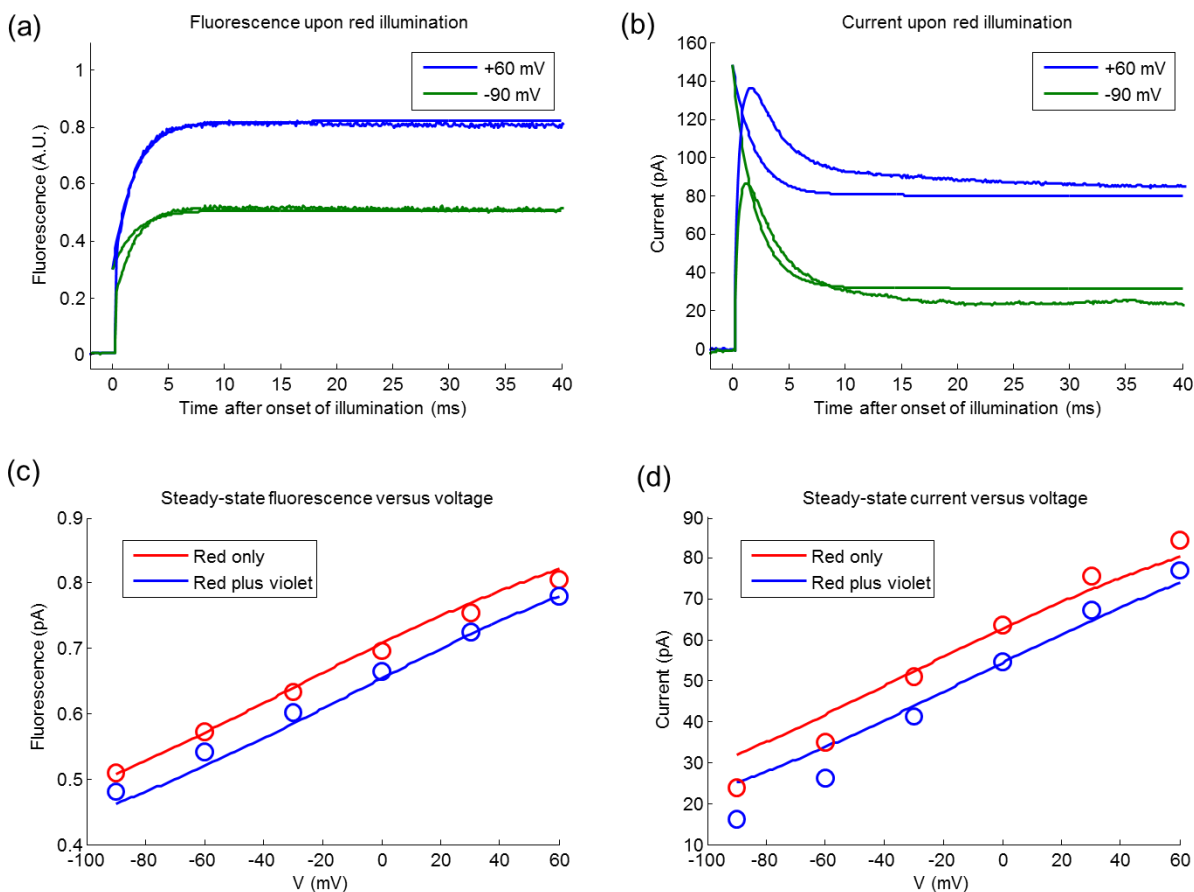


**Figure S13. Fits to the photocycle in Figure 4e.** We modeled the photocycle of Figure 2e quantitatively (see “Model of voltage-dependent fluorescence in Arch” in Supplementary Methods). We reproduced the main features of the data shown in Figure 4d. Panels (a) and (b) show the response of fluorescence and current to the onset of red illumination at -90 mV and +60 mV (see “Time- and voltage-dependent fluorescence in HEK cells” in Methods for experimental details). Fits are shown. The model reproduced the shapes of the transients in both fluorescence and current upon illumination onset. Panels (c) and (d) show steady-state fluorescence and current as a function of membrane voltage under constant 640 nm illumination and under 640 nm + 407 nm illumination. The voltage-dependence of both fluorescence and photocurrent, as well as the decreases in fluorescence and current caused by 407 nm illumination, were recapitulated by our model.



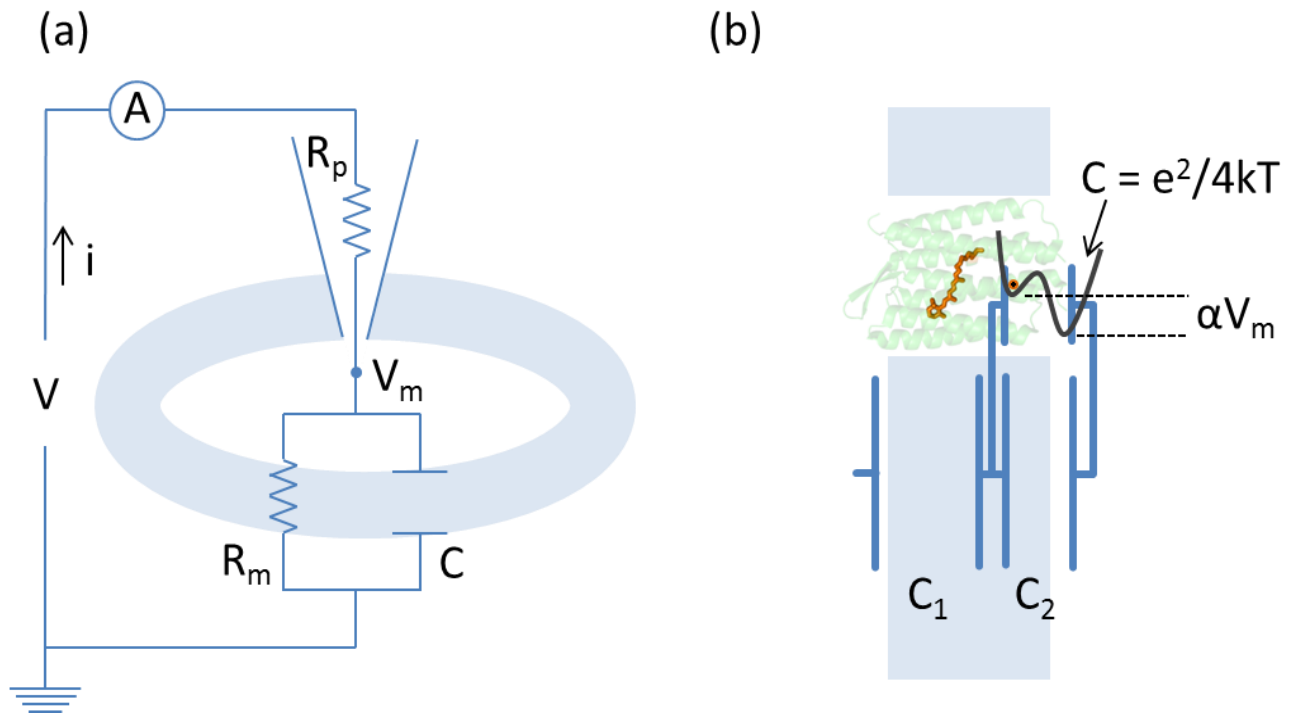


**Figure S14. Electrical models of transient capacitance data.** (a) Equivalent circuit of a cell under patch clamp, showing the pipette resistance,  $R_p$ , the membrane capacitance,  $C$ , and the membrane resistance,  $R_m$ . (b) Voltage-dependent equilibrium of Arch contributes to membrane capacitance by providing a voltage-dependent charge distribution.

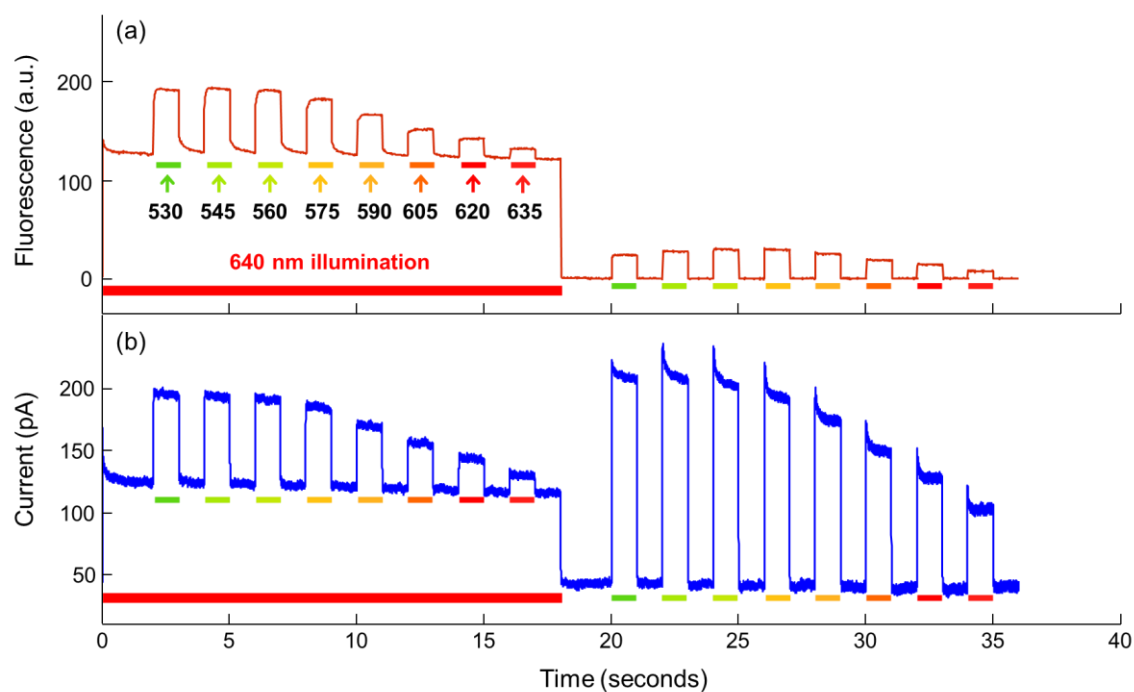


**Figure S15. Effect of intense red illumination on fluorescence and photocurrent action spectra.** A HEK cell expressing WT Arch was held at 0 mV under voltage clamp. (a) Fluorescence excitation spectrum and (b) photocurrent action spectrum of Arch under dim illumination ( $10 \text{ W/cm}^2$ ) in the presence ( $t = 0$  to 18 s) or absence ( $t = 18$  to 36 s) of intense red illumination ( $\sim 1000 \text{ W/cm}^2$ , 640 nm). Addition of intense red light caused slow ( $\sim 200$  ms) transients in fluorescence to appear, while causing the disappearance of slow ( $\sim 300$  ms) transients in photocurrent. Additionally, at wavelengths between 530 and 575 nm, addition of intense red light decreased the total photocurrent. This observation suggests a red light-dependent back-reaction or shortcut in the photocycle. The traces shown are an average of 3 cycles repeated on the same cell. The presence of slow dynamics in the fluorescence (640 nm on) in the absence of slow dynamics in the photocurrent; and slow dynamics in the photocurrent (640 nm off) in the absence of slow dynamics in the fluorescence, suggest that Arch contains transitions that are either spectrally or electrically silent. The presence of such transitions presents a severe challenge for efforts to elucidate the photocycle, and highlights the importance of multimodal spectroscopic and electrical measurements.

## References:

1. Kralj JM, Douglass AD, Hochbaum DR, Maclaurin D, Cohen AE (2012) Optical recording of action potentials in mammalian neurons using a microbial rhodopsin. *Nat Methods* 9:90-95.
2. El-Sayed WSM, *et al.* (2002) Effects of light and low oxygen tension on pigment biosynthesis in halobacterium salinarum, revealed by a novel method to quantify both retinal and carotenoids. *Plant and Cell Physiology* 43:379-383.
3. Enami N, *et al.* (2006) Crystal structures of archaerhodopsin-1 and-2: Common structural motif in archaeal light-driven proton pumps. *J Mol Biol* 358:675-685.
4. Cartailler JP, Luecke H (2003) X-ray crystallographic analysis of lipid-protein interactions in the bacteriorhodopsin purple membrane\*. *Annu Rev Biophys Biomol Struct* 32:285-310.